Electronic Supporting Information

Synthesis and Characterization of Nanocluster-based Silver(I) *tert*-Butylethynide Compound with A Large Second-Harmonic Generation Response

Ting Hu [a, b], Chunli Hu [a], Yuhang Li [a, b], Lingyi Meng [a, b], Yiming Xie [d], Mingyue Liao [d], Guiming Zhong [a, b] and Can-Zhong Lu*[a, b]

a. CAS Key Laboratory of Design and Assembly of Functional Nanostructures, Fujian Provincial Key Laboratory of Nanomaterials, State Key Laboratory of Structural Chemistry, Fujian Institute of Research on the Structure of Matter, Chinese Academy of Sciences, Fuzhou, Fujian Province, P. R. China
b. Xiamen Institute of Rare Earth Materials, Haixi Institute, Chinese Academy of Science, Xiamen 361021, P. R. China
c. College of Materials Science and Engineering, Huaqiao University, Xiamen, Fujian 361021, P. R. China

E-mail: czlu@fjirsm.ac.cn

S9: UV-visible diffuse reflectance spectra and optical band gap of HT-1

S10: Second Harmonic Generation Measurements

S11: Computational Details

S1. Materials and methods

Reagents and solvents obtained from commercial sources were of analytically pure grade and used without further purification. The infrared (IR) spectra were recorded on a Nicolet iS50 spectrometer with ITR mode in the range of 4000–525 cm^{-1} at room temperature. Elemental analyses (C, H, S) were examined with a Vario EL Cube analyzer. Thermogravimetric analyses (TGA) were recorded on a Thermal Analysis Instrument (Mettler-Toledo TGA/DSC 1) from room temperature to 1000 °C with a heating rate of 5 °C/min under air atmosphere. Powder X-ray diffraction (XRD) data were collected on a Rigaku Miniflex 600 diffractometer with Cu Kα radiation in the angular range of 2θ=5-85° with a step size of 0.02°. The Mercury 3.0 program was used to simulate diffraction patterns.[1] Optical diffuse reflectance and UV spectra were recorded at room temperature on an Agilent Cary 5000 UV-vis-NIR spectrophotometer. The reflectance spectra were calculated from absorption spectra using the Kubelka-Munk function: $\alpha/S = (1 - R)^2/2R$, where α is the absorption coefficient, S is the scattering coefficient (which is practically wavelength independent when the particle size is larger than 5 μm), and R is the reflectance.[2] Measurements of the powder frequency-doubling effect were carried out on a sieved sample (70−100 mesh) by means of the modified method of Kurtz and Perry[3] using a fundament wavelength of 1064 nm generated by a Q-switched Nd:YAG laser. Sieved KDP sample in the same size range was used as a reference. ^{1}H magic angle spinning (MAS) NMR experiments were performed on Bruker 400 MHz AVANCE III spectrometer using Hahn-echo pulse under the spinning frequencies of 25 kHz. Recycle delays of 2 s were applied for the acquisition. The chemical shift of ^{1}H was

calibrated using TMS (0 ppm). X-ray photoelectron spectroscopy (XPS) was carried out by an ESCALAB 250Xi spectrometer (Thermo Fisher). Transmission electron microscopy (TEM) measurements were performed on talosF200X microscope. The scanning electron microscopy (SEM) images were measured by a Hitachi SU1510 SEM coupled with an energy-dispersive X-ray (EDX) detector.

S2. Synthesis and single crystal structure analysis

Elemental Polymeric $[^{t}BuC{\equiv}CAg]_n$ was prepared as described previously.[4] Moist $[^{t}BuC{\equiv}CAg]_n$ (≈30 mg) was added to a concentrated DMSO solution (1 mL) of $H_4SiW_{12}O_{40}{\cdot}xH_2O$ (0.144g, 0.05mmol) and $AgCF_3SO_3$ (0.129g, 0.5mmol) in a beaker, and the mixture was stirred for several minutes to form a clear solution. Light green block-like crystals of new compound were isolated (~69%) by diffusion of H_2O into the resulting solution for several days. The formula of the crystal was determined to be $(^{t}BuC{\equiv}CAg)_2(Ag_4SiW_{12}O_{40})(DMSO)_6$ (**HT-1**) on the basis of the combined results of X-ray single crystal structure analysis, elemental analysis and thermogravimetric analysis. Elemental analysis: calcd (%) for $C_{24}H_{54}Ag_6O_{46}S_6SiW_{12}$ (M_r = 4152.54): C 6.94, H 1.31, S 4.63. found: C 6.952, H 1.367, S 5.235.

Crystal data for HT-1: $C_{24}H_{54}Ag_6O_{46}S_6SiW_{12}$ (M = 4152.54 g/mol): Orthorhombic, space group $Pna2_1$(No. 33), a = 27.1669(7) Å, b = 18.3273(4) Å, c = 13.8912(2) Å, V = 6916.4(3) $Å^3$, Z = 4, T = 200 (2) K, μ(Mo-Kα) = 21.807 mm^{-1}, D_{calc} = 3.988 g/cm^3, 264211 reflections measured (5.541° ≤ 2θ ≤ 65.352°), 26590 unique (Rint = 0.0954, Rsigma = 0.0485) which were used in all calculations. The final R_1 was 0.0359 ((I > 2σ(I)) and wR_2 was 0.0761 (all data). CCDC deposit number 1959402. The data can be obtained free of charge from The Cambridge Crystallographic Data Centre via www.ccdc.cam.ac.uk/data_request/cif.

Crystal data were collected on a Xcalibur Eos Gemini diffractometer with Mo-Kα radiation (λ = 0.71073 Å) at 200(2) K. The intensities were corrected for Lorentz and polarization factors, as well as for absorption by the multi-scan method.[5] The structures were solved by the direct method and refined by full-matrix least-squares

fitting on F^2 by SHELX-97,[6] and all non-hydrogen atoms were refined with anisotropic thermal parameters.

Table S1: X-ray crystal data and structure refinement parameters.

Compound	**HT-1**
Empirical formula	$C_{24}H_{54}Ag_6O_{46}S_6SiW_{12}$
Formula weight	4152.54
Crystal system	Orthorhombic
Space group	$Pna2_1$(No. 33)
a [Å]	27.1669(7)
b [Å]	18.3273(4)
c [Å]	13.8912(2)
α [°]	90
β [°]	90
γ [°]	90
V[Å^3]	6916.4(3)
Z	4
D_{calc}(g/cm3)	3.988
μ(Mo-Kα)(mm^{-1})	21.807
F(000)	7384.0
Reflections collected	264211
Independent reflections	26590
Parameters	874
Goodness-of-fit	1.048
$R_1[I>2s(I)]$[a]	0.0359
wR_2(all data)[b]	0.0761

[a] $R_1 = \sum||F_o| - |F_c||/\sum|F_o|$. [b] $wR_2 = \{\sum[w(F_o^2 - F_c^2)^2]/\sum[w(F_o^2)^2]\}^{1/2}$

Table S2. Selected bond lengths **(**Å**)** for **HT-1**.

HT-1					
C1≡C2	1.23(2)	Ag2···Ag4	2.882(2)	Ag4-O36#3	2.448(9)
Ag1-C1	2.26(1)	Ag2···Ag5	2.943(2)	Ag5-C1	2.19(1)
Ag1-C2	2.55(1)	Ag3-C7	2.24(1)	Ag5-O44	2.55(1)
Ag1-O21	2.591(9)	Ag3-C8	2.41(1)	Ag5-O45	2.24(1)
Ag1-O41	2.29(1)	Ag3-O22	2.52(1)	Ag5···Ag6	3.323(2)
Ag1-O25#1	2.343(9)	Ag3-O42	2.25(1)	Ag6-O43	2.48(1)
Ag1···Ag2	3.021(2)	Ag3-O6#2	2.397(9)	Ag6-O44	2.36(1)
Ag2-C1	2.09(1)	Ag4-C7	2.22(1)	Ag6-O45	2.57(2)
Ag2-C7	2.11(1)	Ag4-O43	2.35(1)	Ag6-O46	2.35(1)
Ag2···Ag3	3.013(2)	Ag4-O46	2.38(1)		

[a] Symmetry transformations used to generate equivalent atoms:

For **HT-1**: #1 $-x+2, -y+1, z+0.5$; #2 $-x+1.5, y-0.5, z-0.5$; #3 $-x+1.5, y-0.5, z+0.5$.

S3: View of the three-dimensional crystal structure of HT-1

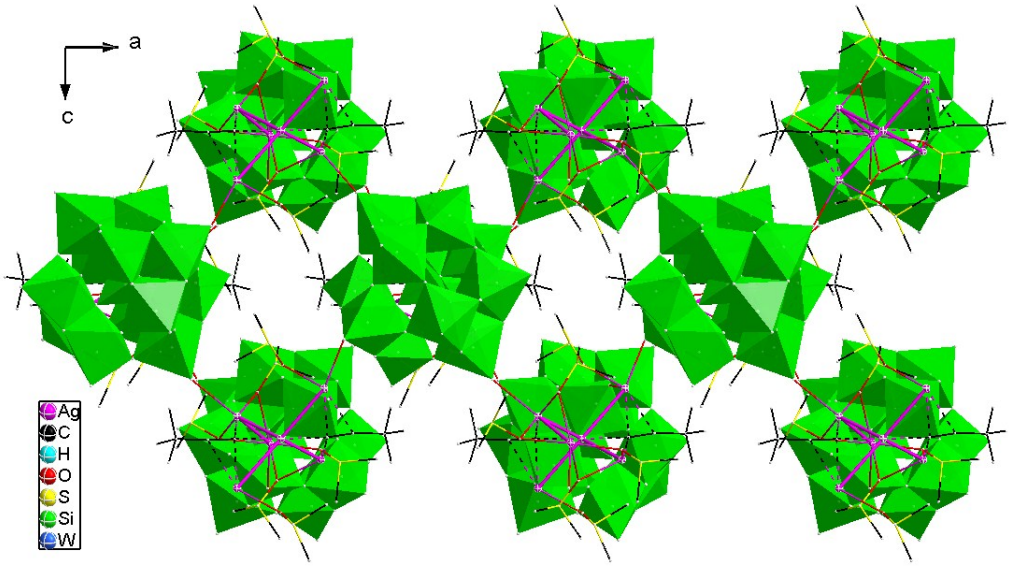

(a)

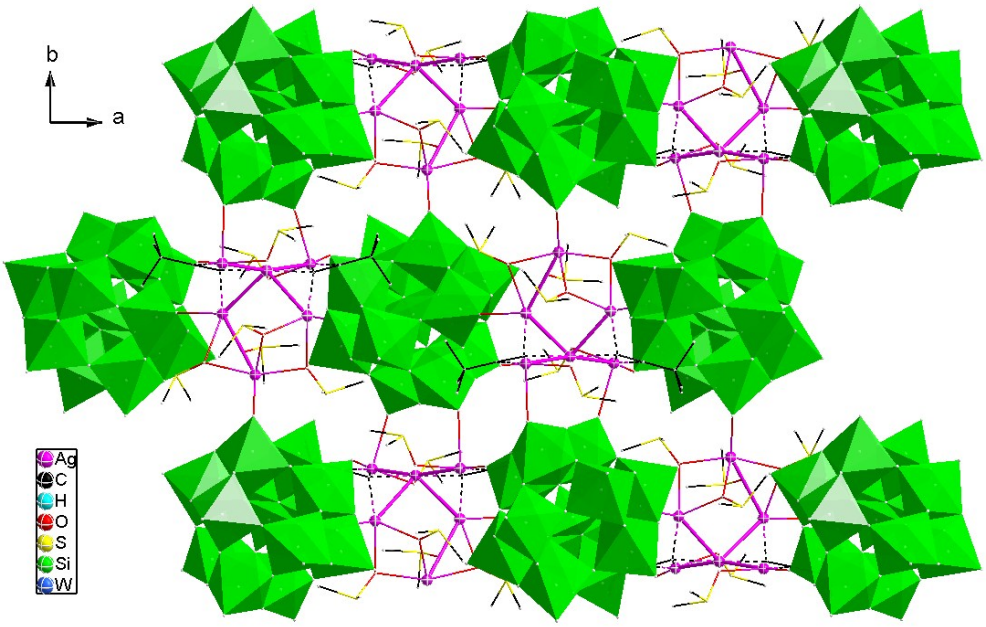

(b)

Fig. S1. View of the three-dimensional coordination structure of **HT-1** along the *b* axis (a) and *c* axis (b). The H atoms are omitted for clarity.

S4: Powder X-ray Diffraction (PXRD)

The PXRD patterns for **HT-1** are presented in Figure S2, and the observed XRD patterns agree with those simulated from their structures.

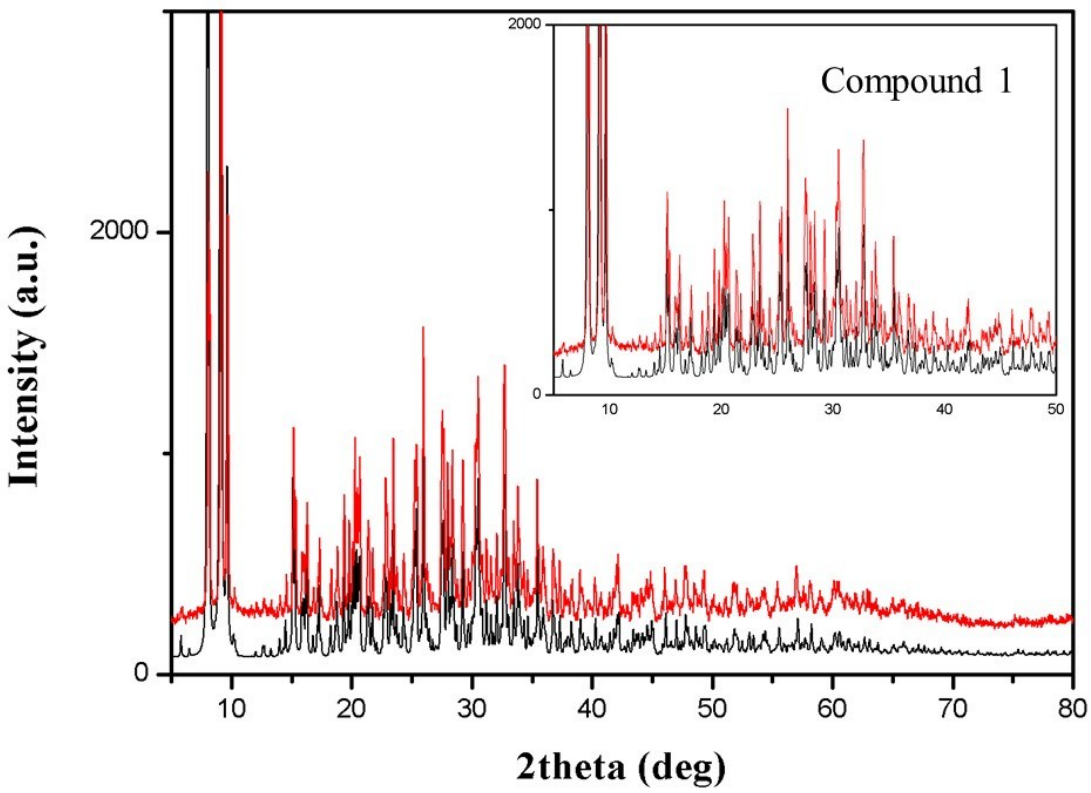

Fig. S2. Experimental (red) and simulated (black) X-ray powder diffraction patterns for **HT-1.**

S5: The FT-IR spectrum

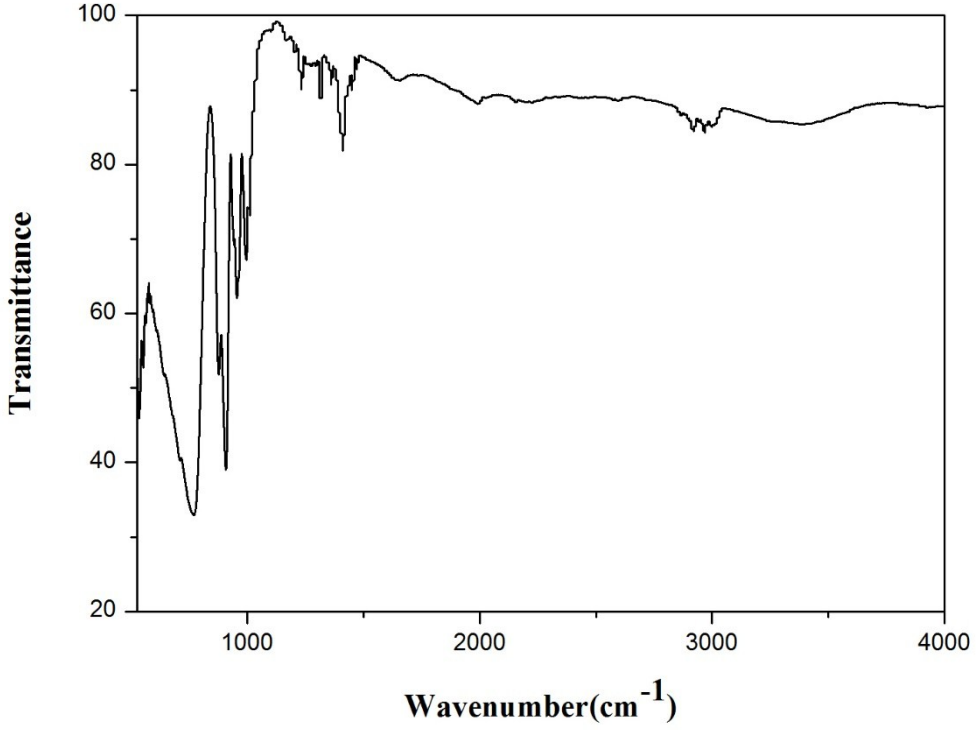

Fig. S3. The infrared spectra of **HT-1**.

S6: Solid-State NMR

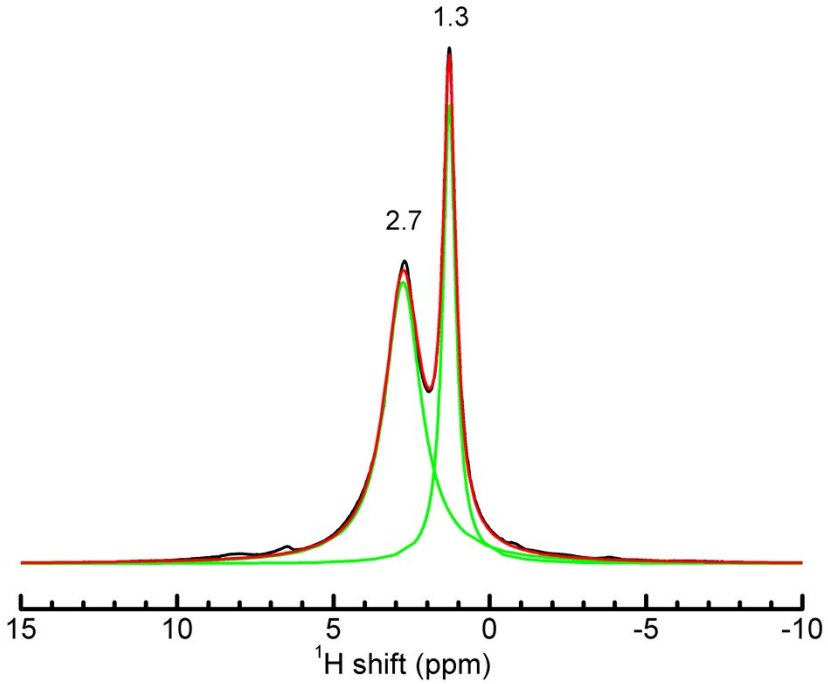

Fig. S4. The ^{1}H MAS NMR spectrum of **HT-1**. The ^{1}H chemical shift of the ^{t}BuC≡C$^-$ groups is 1.3 ppm. The ^{1}H chemical shift of DMSO ligands is 2.7 ppm.

S7: Thermogravimetric Analyses (TGA)

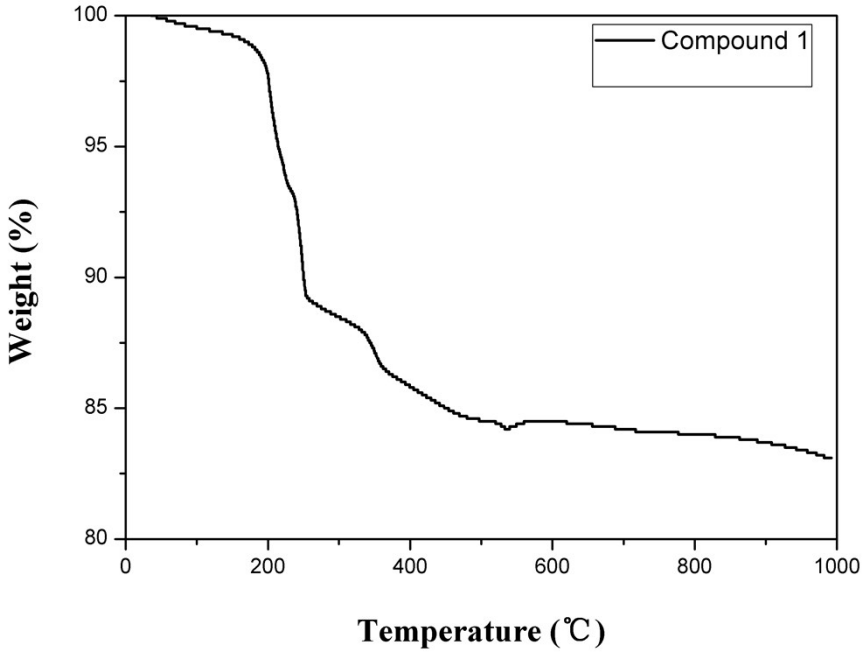

Fig. S5. The thermogravimetric analyses curve of **HT-1** with a heating rate of 5°C/min under air atmosphere.

S8: UV-visible absorption spectra of HT-1

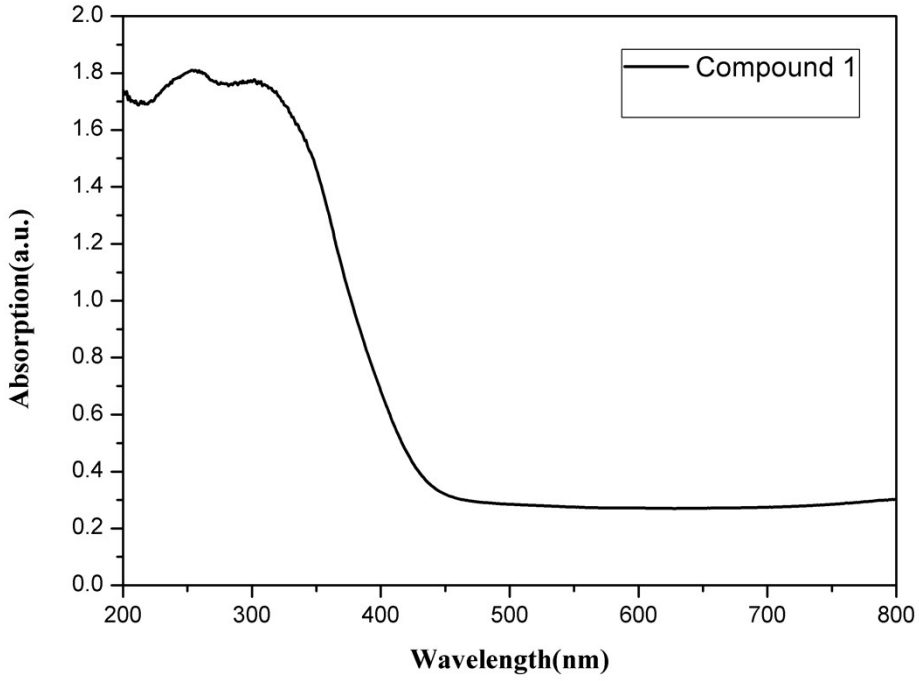

Fig. S6: UV-visible absorption spectra of **HT-1**.

S9: UV-visible diffuse reflectance spectra and optical band gaps of HT-1

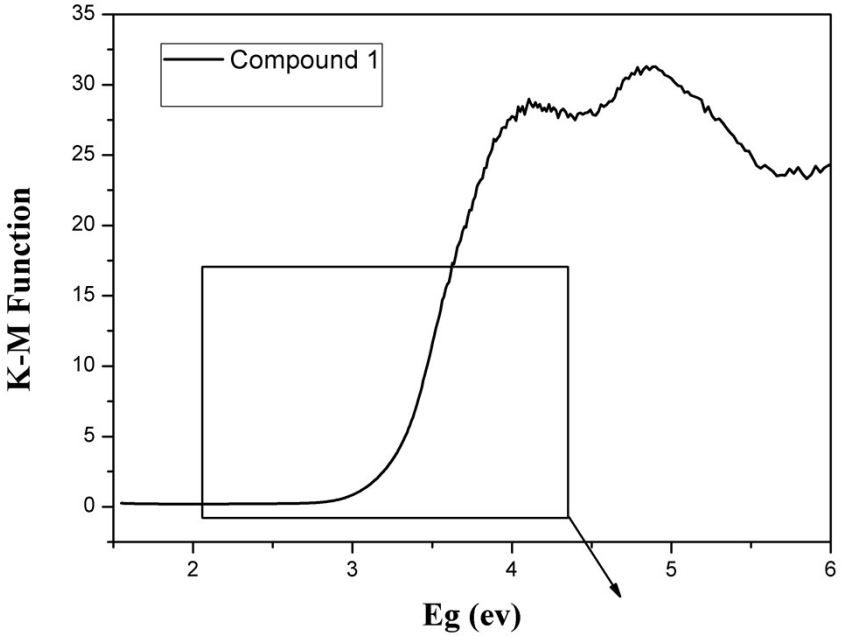

Fig. S7. UV-visible diffuse reflectance spectra.

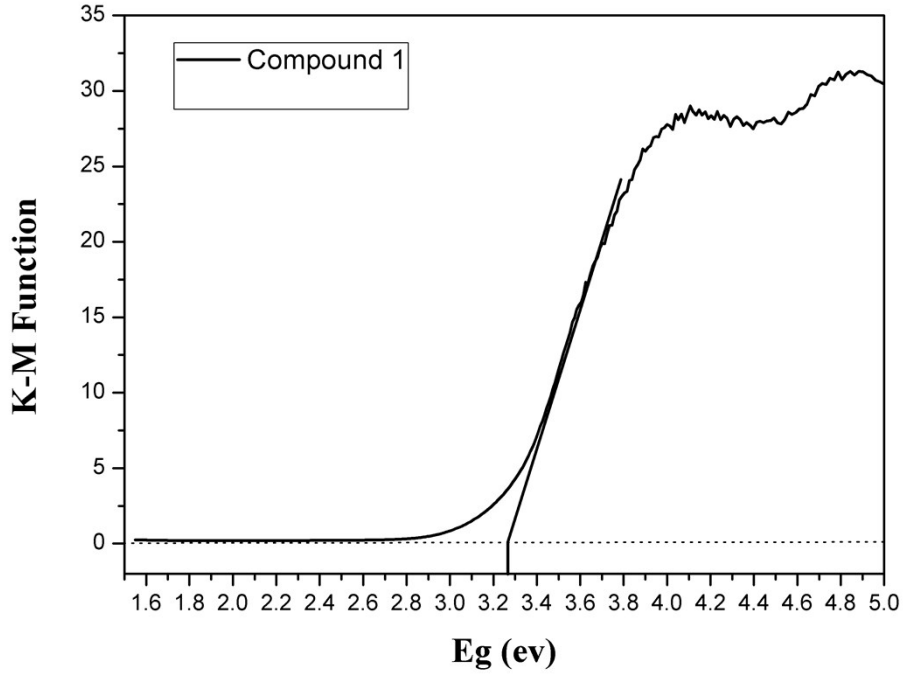

Band gap (eV) of **HT-1**: 3.27

Fig. S8. Optical band gap of **HT-1**.

S10: Powder Second Harmonic Generation (SHG) Measurements

The Powder SHG measurements of **HT-1** and KH_2PO_4 (KDP) standard samples were performed with a Q-switched Nd: YAG solid-state laser at the wavelength of 1064 nm, according to the method from Kurtz and Perry.[7] Because SHG efficiencies are known to strongly depend on the particle size, polycrystalline samples of **HT-1** were ground and sieved into six particle size ranges: 25-45, 45-62, 62-75, 75-109, 109-150, and 150-212 μm. To make relevant comparisons with known SHG materials, crystalline KDP was also ground and sieved into the same particle size ranges as the comparison reference. The **HT-1** samples were pressed into some 1 mm thick aluminum holders containing the hole with 8 mm in diameter and covered by glass microscope cover slides. Then the samples were placed in a light-tight box and irradiated with a pulsed laser one by one, which from an optical parametric oscillator laser pumped with a Q-switched Nd: YAG laser of wave-length 1064 nm. In order to avoid the affection of background flash-lamp, a cut-off filter was employed, and an interference filter (530 ± 10 nm) was used to select the second harmonic for detection with a photomultiplier tube attached to a RIGOL DS1052E 50-MHz oscilloscope. The above procedures were repeated using the reference sample KDP and the proportion of the second harmonic intensity signal outputs between **HT-1** and KDP were calculated. All of the experiments were performed without index-matching fluid.

S11. Computational Details

Single-crystal structural data of **HT-1** was used for the theoretical calculations. The electronic structures and optical properties were calculated by using a plane-wave pseudopotentials method within density functional theory (DFT) implemented in the total energy code of CASTEP.[8] For the exchange-correlation functional, we chose Perdew−Burke−Ernzerhof (PBE) in the generalized gradient approximation (GGA).[9] The interactions between the ionic cores and the electrons were described by the norm-conserving pseudopotential.[10] The following valence-electron configurations were considered in the computation: O-$2s^2 2p^4$, Ag-$4s^2 4p^6 4d^{10} 5s^1$, W-$5d^4 6s^2$, Si-$3s^2 3p^2$, S-$3s^2 3p^4$, C-$2s^2 2p^2$ and H-$1s^1$. The number of plane waves included in the basis sets

was determined by a cutoff energy of 765 eV. Monkhorst−Pack k-point sampling of 1 × 1 × 2 was used to perform numerical integration of the Brillouin zone for **HT-1**. During the optical property calculations, more than 2600 empty bands were set to ensure the convergence of SHG coefficients for **HT-1**.

The calculations of second-order NLO properties were based on length-gauge formalism within the independent particle approximation.[11] The second-order NLO susceptibility can be expressed as

$$\chi abc \text{ L } (-2\omega; \omega, \omega) = \chi abc \text{ L, e } (-2\omega; \omega, \omega) + \chi abc \text{ L, i } (-2\omega; \omega, \omega)$$

where the subscript L denotes the length gauge; χabc L, e and χabc L, i give the contributions to χabc L from interband processes and intraband processes, respectively.

To show the distribution of the quantum states relevant to SHG process, the SHG-weighed electron density analysis was implemented. In the scheme, the considered SHG coefficient is "resolved" into each band/orbital, and based on the "band-resolved" method, each band/orbital's contribution to a specific SHG coefficient can be identified. Using the normalized effective SHG for each band/orbital as a weighting coefficient, and summing all the SHG-weighted bands/orbitals in VB or CB over the different k points in the space, the SHG-weighed electron density can be obtained.[12]

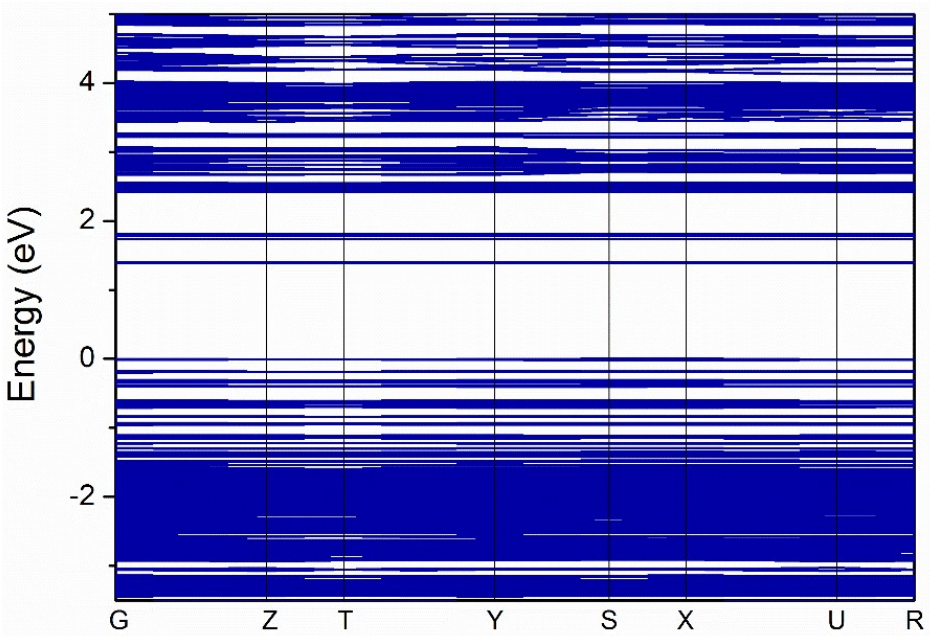

Fig. S9. The calculated band structure of **HT-1.**

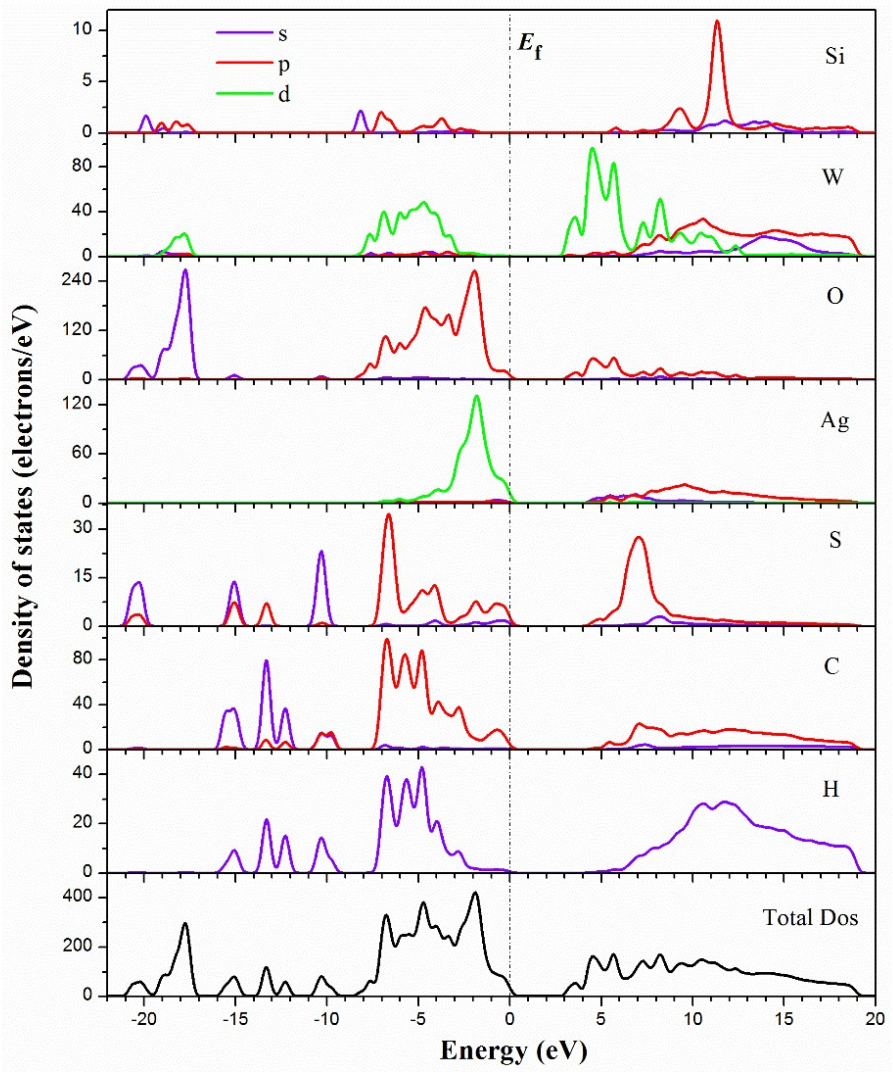

Fig. S10. The calculated total and partial density of states of **HT-1.**

Reference

1 C. F. Macrae, I. J. Bruno, J. A. Chisholm, P. R. Edgington, P. McCabe, E. Pidcock, L. Rodriguez-Monge, R. Taylor, J. v. d. Streek and P. A. Wood, *J. Appl. Crystallogr*., 2008, 41, 466-470.

2 W. M. Wendlandt and H. G. Hecht, *Reflectance Spectroscopy*, Interscience, New York, 1966.

3 (*a*) K. E. Rieckhoff and W. L. Peticolas, *Science*., 1965, 147, 610-611; (*b*) S. K. Kurtz and T. T. Perry, *J. Appl. Phys*., 1968, 39, 3798-3813.

4 L. Zhao, W.-Y. Wong and T. C. W. Mak, *Chem- Eur. J.*, 2006, 12, 4865-4872.

5 *CrystalClear, Version 1.3.5*, Rigaku Corp., Woodlands, TX, 1999.

6 G. M. Sheldrick, *SHELXTL*, *Crystallographic Software Package*, *Version 5.1*, Bruker-AXS, Madison, WI, 1998.

7 S. K. Kurtz and T. T. Perry, *J Appl Phys.*, 1968, 39, 3798-3813.

8 (a) V. Milman, B. Winkler, J. A. White, C. J. Pickard, M. C. Payne, E. V Akhmatskaya and R. H. Nobes, *Int. J. Quantum Chem.*, 2000, **77**, 895. (b) M. D. Segall, P. J. D. Lindan, M. J. Probert, C. J. Pickard, P. J Hasnip, S. J. Clark and M. C. Payne, *J. Phys.: Condens. Matter.*, 2002, **14**, 2717.

9 J. P. Perdew, K. Burke and M. Ernzerhof, *Phys. Rev. Lett.*, 1996, **77**, 3865.

10 J. S. Lin, A. Qteish, M. C. Payne and V. V. Heine, *Phys.Rev.B: Condens. Matter Mater. Phys.*, 1993, **47**, 4174.

11 J. L. Cabellos, B. S. Mendoza, M. A. Escobar, F. Nastos and J. E. Sipe, *Phys. Rev. B: Condens. Matter.*, 2009, **80**, 155205.

12 C. H. Lo and M. H. Lee, *Master Thesis.*, Taiwan, 2005, 29.